An exact Riemann solver for one-dimensional multi-material elastic-plastic flows with Mie-Grüneisen equation of state

Li Liu[1], Jun-bo Cheng [1,*], Jiequan Li [1]

June 14, 2019

Abstract

The Riemann problem for one-dimensional multi-material elastic-plastic flows with the Mie-Grüneisen EOS, hypo-elastic constitutive model and the von Mises' yielding condition is studied in this paper. Through a detailed analysis of the Jacobian matrix and relations across different type of waves, an exact Riemann solver is constructed with totally thirty-six possible cases of structure. Some useful results are also obtained in the analysing, for example, the sonic speed experiences a significant jump when the material is yielding and the plastic wave is always faster than the elastic wave. More over, an exact Riemann solver is also deduced for the half Riemann problem. A lot of examples show that, the results taken by the exact Riemann solver are in good agreement with those computed by the mumerical method.

1 Introduction

In this paper, an exact Riemann solver is built for one-dimensional multi-material elastic-plastic flows with the Mie-Grüneisen EOS, hypo-elastic constitutive model [**?**] and the von Mises' yielding condition.

The elastic-plastic flow is used to describe the deformation process of solid materials under strong dynamics loading, such as explosive or high-speed impact. The simulation of elastic-plastic flows has important application backgrounds, especially in the Implosion Dynamics weapon and Inertial Confine Fusion (ICF). The first try of simulating the elastic-plastic flows was given by Wilkins [**?**] in 1960s.

In the development history of hydrodynamic numerical methods, the exact Riemann solver has played a very important role as it not only can give a guide and reference to the construction of approximate Riemann solvers, but also can be used to determine the convergence and stability of numerical schemes. However, building the exact Riemann solver for 1D elastic-plastic flows is not that easy. Comparing with the governing equations system of 1D pure fluids, for 1D elastic-plastic flows, there are two more equations: a non-conservative constitutive equation and the von Mises yielding condition. The non-conservative character of the constitutive equation increases the difficulty in constructing Riemann solvers, while the von Mises yielding condition may leads to more non-linear waves in the structure of Riemann solvers. Moreover, in a general way, the equation of state(EOS) for solid materials is more complex than that for pure fluids, which directly increases the difficulty in solving the Riemann problem.

For the elastic-plastic flow with the hypo-elastic constitutive model and the von Mises' yielding condition, some approximate Riemann solvers[**?**, **?**, **?**, **?**] have been developed recently. However, for the exact Riemann solver, the research is relatively few, and them are only considered with simple constitutive models and simple EOSs. For example, Garaizar [**?**] and Miller [**?**] introduced an exact Riemann solver for elastic or hyper-elastic materials, Gao and Liu [**?**, **?**] firstly considered the yielding effect and developed an exact elastic-perfectly plastic solid Riemann solver, but the EOS used by them is very simple: in the elastic state, the material derivative of pressure is the linear function of the strain rate, which means the energy equation is not necessary; in the plastic state, a linear "stiffened-gas" EOS was used. All these makes easily deduce the relation across a non-linear wave. Although there are many cases considered in their works [**?**, **?**], for every case, they can easily obtain the exact solution. But for many engineering problems, the EOS is more complex, and the energy equation has to be included during simulating. For these engineering solid problems with a complex constitutive and a complex EOS, such as the Mie-Grüneisen EOS, up to now, there is no exact Riemann solution.

In this paper, we want to construct an exact Riemann solver for the system of 1D elastic-plastic flows with the Mie-Grüneisen EOS, the hypo-elastic constitutive model and the von Mises' yielding condition. As every knows, the Mie-Grüneisen EOS is complex and is used widely in many engineering problems, which makes the energy equation must be included in the system of elastic-plastic flows and so we have to use some special methods to resolve the rarefaction wave. Otherwise, we analyse the Jacobian matrix and find, in the wave structures of Riemann solvers, there may be three to five waves, including one contact wave and other two to four non-linear waves. These nonlinear waves may be elastic shock waves, elastic rarefaction waves, plastic shock waves or plastic rarefaction waves. Moreover, elastic wave runs always faster than the followed plastic wave. So there are thirty-six possible cases of the wave structures in the Riemann solver.

This paper is organized as follows. In section 2, we introduce the governing equations to be studied. In section 3, the Riemann problem and the relations for every wave type (contact wave, shock wave and rarefaction wave) are derived. Then, the exact Riemann solver is given in section 4. The half Riemann problem and its solver is introduced in section 5. Some numerical examples are presented to validate the method in section 6. Conclusions are shown in section 7.

2 Governing equations

In this paper, the elastic energy is not included in the total energy. The exclution of the elastic energy is usual for practical engineering problems [**?**] and is different from that in Ref.[**?**].

2.1 Motion equations

For a continuous one-dimensional homogeneous solid, the motion equations in differential form are

$$\partial_t \mathbf{U} + \partial_x \boldsymbol{F}(\mathbf{U}) = 0,\ x \in\ \Omega \subset \mathbf{R},\ t > 0,$$

where

$$\mathbf{U} = \begin{bmatrix} \rho \\ \rho u \\ \rho E \end{bmatrix}, \quad \mathbf{F} = \begin{bmatrix} \rho u \\ \rho u^2 - \sigma \\ (\rho E - \sigma) u \end{bmatrix}, \tag{2.1}$$

ρ, u, σ and E are the density, velocity in $x-$direction, Cauchy stress and total energy per unit volume, respectively, E has the relation with specific internal energy e as

$$E = e + \frac{1}{2}u^2, \tag{2.2}$$

$$\sigma = -p + s_{xx}, \tag{2.3}$$

where p and s_{xx} denote hydrostatic pressure and deviatoric stress in the $x-$ direction, respectively.

2.2 The equation of state (EOS)

The relation of the pressure with the density and the specific internal energy is gotten from the equation of state (EOS). In this paper, we consider the Mie-Grüneisen EOS,

$$p(\rho, e) = \rho_0 a_0^2 f(\eta) + \rho_0 \Gamma_0 e, \tag{2.4}$$

where $f(\eta) = \frac{(\eta-1)(\eta-\Gamma_0(\eta-1)/2)}{(\eta-s(\eta-1))^2}$, $\eta = \frac{\rho}{\rho_0}$, ρ_0, a_0, s and Γ_0 are constant parameters of the Mie-Grüneisen EOS.

2.3 The constitutive relation

Hooke's law is used here to describe the relationship between the deviatoric stress and the strain,

$$\dot{s}_{xx} = 2\mu \left(\dot{\varepsilon}_x - \frac{1}{3}\frac{\dot{V}}{V} \right), \tag{2.5}$$

where μ is the shear modulus, V is the volume, and the dot means the material time derivative,

$$\dot{()} = \frac{\partial()}{\partial t} + u\frac{\partial()}{\partial t}, \tag{2.6}$$

and

$$\dot{\varepsilon}_x = \frac{\partial u}{\partial x}, \quad \frac{\dot{V}}{V} = \frac{\partial u}{\partial x}. \tag{2.7}$$

By using Eq.(2.7), Eq.(2.5) can be rewritten as

$$\frac{\partial s_{xx}}{\partial t} + u\frac{\partial s_{xx}}{\partial t} = \frac{4}{3}\mu\frac{\partial u}{\partial x}. \tag{2.8}$$

2.4 The yielding condition

The Von Mises' yielding condition is used here to describe the elastic limit. In one spatial dimension, the von Mises' yielding criterion is given by

$$|s_{xx}| \leq \frac{2}{3}Y_0, \tag{2.9}$$

where Y_0 is the yield strength of the material in simple tension.

3 The Riemann problem

The Riemann problem for the 1D time dependent elastic-plastic equations is given as follows:

$$\begin{cases} \partial_t\rho + \partial_x(\rho u) = 0, \\ \partial_t(\rho u) + \partial_x(\rho u^2 + p - s_{xx}) = 0, \\ \partial_t(\rho E) + \partial_x\left[(\rho E + p - s_{xx})u\right] = 0, \\ \partial_t s_{xx} + u\partial_x s_{xx} - \dfrac{4}{3}\partial_x u = 0, \\ |s_{xx}| \leq \dfrac{2}{3}Y_0, \\ Q(x, t=0) = \begin{cases} Q_L, \text{ if } x < 0, \\ Q_R, \text{ if } x \geq 0, \end{cases} \end{cases} \tag{3.1}$$

where $Q = (\rho, \rho u, \rho E, s_{xx})^T$.

The above equations are just for the elastic status of the solid material. If the material are in the plastic state, the above equations can be simplified and correspondingly the jacobian matrix and sonic velocity are different. We will discuss them separately.

3.1 Elastic state

3.1.1 Jacobian matrix in elastic regions

For the Mie-Grüneisen EOS, if the material is not yielding,

$$|s_{xx}| < \frac{2}{3}Y_0, \tag{3.2}$$

the system (3.1) can be written as

$$\partial_t\mathbf{Q} + \mathbf{J}_e(\mathbf{Q})\partial_x\mathbf{Q} = 0, \tag{3.3}$$

where $Q = (\rho, \rho u, \rho E, s_{xx})$, and the Jacobian matrix is

$$\mathbf{J}_e(Q) = \begin{bmatrix} 0 & 1 & 0 & 0 \\ -u^2 + \frac{\partial p}{\partial \rho} + \Gamma(\frac{u^2}{2} - e) & u(2-\Gamma) & \Gamma & -1 \\ (\Gamma(\frac{u^2}{2} - e) - e - \frac{u^2}{2} + \frac{\sigma}{\rho} + \frac{\partial p}{\partial \rho})u & -\Gamma u^2 - \frac{\sigma}{\rho} + \frac{u^2}{2} + e & (1+\Gamma)u & -u \\ \frac{4}{3}\mu\frac{u}{\rho} & -\frac{4}{3}\mu\frac{1}{\rho} & 0 & u \end{bmatrix}, \tag{3.4}$$

where $\Gamma = \frac{\Gamma_0 \rho_0}{\rho}$.

The eigenvalues of $\mathbf{J}_e(\mathbf{Q})$ are given as

$$\lambda_1 = \lambda_2 = u, \quad \lambda_3 = u - c_e, \quad \lambda_4 = u + c_e, \tag{3.5}$$

where c_e means the sonic speed of the solid in the elastic state,

$$\begin{cases} c_e = \sqrt{a^2 - \dfrac{\rho_0}{\rho^2}\Gamma_0 s_{xx} + \dfrac{4}{3}\dfrac{\mu}{\rho}}, \\ a^2 = \dfrac{\partial p}{\partial \rho} + \dfrac{p}{\rho^2}\dfrac{\partial p}{\partial e} = a_0^2 \dfrac{\partial f}{\partial \eta} + \dfrac{p}{\rho^2}\rho_0 \Gamma_0. \end{cases} \tag{3.6}$$

The corresponding right eigenvectors are

$$r_1 = \begin{bmatrix} \frac{1}{b_1} \\ \frac{u}{b_1} \\ 0 \\ 1 \end{bmatrix}, \quad r_2 = \begin{bmatrix} -\frac{\Gamma}{b_1} \\ -\frac{\Gamma u}{b_1} \\ 1 \\ 0 \end{bmatrix}, \quad r_3 = \frac{1}{\phi^2}\begin{bmatrix} 1 \\ u - c_e \\ h - u c_e \\ \phi^2 \end{bmatrix}, \quad r_4 = \frac{1}{\phi^2}\begin{bmatrix} 1 \\ u + c_e \\ h + u c_e \\ \phi^2 \end{bmatrix}, \tag{3.7}$$

where

$$b_1 = \frac{\partial p}{\partial \rho} - \Gamma E, \quad h = E + \frac{p - s_{xx}}{\rho}, \tag{3.8}$$

and

$$\phi^2 = a^2 - \frac{\rho_0}{\rho^2}\Gamma_0 s_{xx} - c_e^2 = -\frac{4\mu}{3}\frac{1}{\rho}. \tag{3.9}$$

3.1.2 A relation between ρ and s_{xx}

Thanks to (2.6), the equations of the density and the deviatoric stress in Eq.(3.1) can be written as

$$\frac{\partial u}{\partial x} = -\frac{1}{\rho}\frac{d\rho}{dt}, \tag{3.10}$$

and

$$\frac{ds_{xx}}{dt} = \frac{4}{3}\mu \frac{\partial u}{\partial x}. \tag{3.11}$$

Substituting (3.10) into (3.11) yields

$$\frac{ds_{xx}}{dt} = -\frac{4}{3}\mu \frac{1}{\rho}\frac{d\rho}{dt}. \tag{3.12}$$

Integrate the above equation from the data in front of a wave to the data behind the wave and perform some simple algebraic manipulations, one can get

$$s_{xx} + \frac{4}{3}\mu \ln(\rho) = \text{constant} \tag{3.13}$$

This relation always hold in the elastic state.

3.1.3 Relations across the contact wave

For a system without molecular diffusion, there is no materials convecting across the contact wave or interface, so the velocities on two sides of the discontinuity are always equal. This can also be verified by the eigenvectors in Eq.(3.7) and Eq.(3.62).

Using $\mathbf{Q}_L^*$ and $\mathbf{Q}_R^*$ to denote the two data states connected the contact wave, where $\mathbf{Q} = (\rho, u, p, s_{xx})$.

Thanks to Eq.(3.7), for the λ_1-wave we have

$$\frac{d\rho}{\frac{1}{b_1}} = \frac{d\rho u}{\frac{u}{b_1}} = \frac{d\rho E}{0} = \frac{ds_{xx}}{1}. \tag{3.14}$$

From the above equations, we can easily deduce that

$$du = 0, \quad d(s_{xx} - p) = 0, \tag{3.15}$$

which means

$$u_L^* = u_R^*, \tag{3.16}$$

and

$$\sigma_{x,L}^* = \sigma_{x,R}^*, \tag{3.17}$$

where $()_L^*$ and $()_R^*$ denote () in the region of $\mathbf{Q}_L^*$ and $\mathbf{Q}_R^*$, respectively. Here we do not show the details of the derivation for a simple presentation.

Similarly, for the λ_2-wave one has

$$\frac{d\rho}{\frac{-\Gamma}{b_1}} = \frac{d\rho u}{\frac{-u\Gamma}{b_1}} = \frac{d\rho E}{1} = \frac{ds_{xx}}{0}. \tag{3.18}$$

From the above equations, we can easily deduce that

$$du = 0, \quad dp = 0, \quad ds_{xx} = 0, \tag{3.19}$$

which means

$$u_L^* = u_R^*, \tag{3.20}$$

$$p_L^* = p_R^*, \quad s_{xx,L}^* = s_{xx,R}^*. \tag{3.21}$$

From Eq.(3.21), we get that

$$\sigma_{x,L}^* = \sigma_{x,R}^*. \tag{3.22}$$

At last, for the λ_1 and λ_2 waves, one can find that the following two relations always hold:

$$u_L^* = u_R^*, \quad \sigma_{x,L}^* = \sigma_{x,R}^*. \tag{3.23}$$

For convenience, we define

$$s^* = u_L^* = u_R^*. \tag{3.24}$$

where s^* denotes the velocity of the contact wave.

3.1.4 Relations across rarefaction waves

Left-going rarefaction wave Across the left wave associated with λ_3-wave, ($\lambda_3 = u - c_e$), we have

$$\frac{d\rho}{1} = \frac{d(\rho u)}{u - c_e} = \frac{d(\rho E)}{h - uc_e} = \frac{ds_{xx}}{-\frac{4\mu}{3}\frac{1}{\rho}}. \tag{3.25}$$

which leads to

$$\mathrm{d}u = -\frac{c_e}{\rho}\mathrm{d}\rho, \tag{3.26}$$

$$\mathrm{d}E = -\frac{\sigma + \rho u c_e}{\rho^2}d\rho, \tag{3.27}$$

$$\mathrm{d}s_{xx} = -\frac{4}{3}\frac{\mu}{\rho}d\rho. \tag{3.28}$$

Using (2.4), one can get

$$dE = de + udu. \tag{3.29}$$

Substituting (3.26) and (3.27) into the above equation yields

$$de = -\frac{\sigma}{\rho^2}d\rho = \frac{p - s_{xx}}{\rho^2}d\rho. \tag{3.30}$$

Thanks to (2.4), one can get

$$dp = \frac{\partial p}{\partial \rho} d\rho + \frac{\partial p}{\partial e} de = a_0^2 \frac{\partial f}{\partial \eta} d\rho + \rho_0 \Gamma_0 de, \tag{3.31}$$

Substituting (3.30) into the above equation yields

$$dp = \left(a_0^2 \frac{\partial f}{\partial \eta} + \frac{p}{\rho^2} \rho_0 \Gamma_0 - \frac{\rho_0}{\rho^2} \Gamma_0 s_{xx} \right) d\rho. \tag{3.32}$$

The above equation can be rewritten as a differential equation of $p(\rho)$

$$p'(\rho) - \lambda \frac{p}{\rho^2} = f_2(\rho), \tag{3.33}$$

where

$$\lambda = \rho_0 \Gamma_0 \quad f_2(\rho) = a_0^2 \frac{\partial f}{\partial \eta} - \lambda \frac{s_{xx}(\rho)}{\rho^2}. \tag{3.34}$$

By integrating (3.33) across the left rarefaction wave, the pressure can be solved out as

$$p e^{\frac{\lambda}{\rho}} - \int f_2(\rho) e^{\frac{\lambda}{\rho}} d\rho = \text{constant}. \tag{3.35}$$

Integrating (3.26) across the left rarefaction wave yields

$$u + \int \frac{c_e}{\rho} d\rho = \text{constant}. \tag{3.36}$$

Right-going rarefaction wave

Across the right wave associated with λ_4-wave, ($\lambda_3 = u + c_e$), we have

$$\frac{d\rho}{1} = \frac{d(\rho u)}{u + c_e} = \frac{d(\rho E)}{h + u c_e} = \frac{d s_{xx}}{-\frac{4\mu}{3} \frac{1}{\rho}}. \tag{3.37}$$

which leads to

$$\mathrm{d}u = \frac{c_e}{\rho} \mathrm{d}\rho, \tag{3.38}$$

$$\mathrm{d}E = -\frac{\sigma + \rho u c_e}{\rho^2} d\rho, \tag{3.39}$$

$$\mathrm{d}s_{xx} = -\frac{4}{3} \frac{\mu}{\rho} d\rho. \tag{3.40}$$

By using the same method, one can get

$$p e^{\frac{\lambda}{\rho}} - \int f_2(\rho) e^{\frac{\lambda}{\rho}} d\rho = \text{constant}. \tag{3.41}$$

$$u - \int \frac{c_e}{\rho} d\rho = \text{constant}. \tag{3.42}$$

3.1.5 Relations across shock waves

Now we consider a shock wave moving with the speed of s. The data in front of the shock is $(\rho_1, u_1, p_1, s_{xx1})$ and that after the shock is $(\rho_2, u_2, p_2, s_{xx2})$.

We transform the equations to a frame of reference moving with the shock and the Rankine-Hugoniot Conditions give

$$\rho_2 (u_2 - s) = \rho_1 (u_1 - s), \tag{3.43}$$

$$\rho_2 u_2 (u_2 - s) = \rho_1 u_1 (u_1 - s) + \sigma_2 - \sigma_1, \tag{3.44}$$

$$\rho_2 E_2 (u_2 - s) = \rho_1 E_1 (u_1 - s) + \sigma_2 u_2 - \sigma_1 u_1. \tag{3.45}$$

Substituting (3.43) into (3.44) yields

$$\rho_1(u_2 - u_1)(u_1 - s) = \sigma_2 - \sigma_1. \tag{3.46}$$

From (3.43), one has

$$u_1 - s = \frac{(u_1 - u_2)\rho_2}{\rho_2 - \rho_1}, \tag{3.47}$$

then subtituting it into (3.46) yields

$$-t(u_2 - u_1)^2 = \sigma_2 - \sigma_1, \tag{3.48}$$

where $t = \frac{\rho_1\rho_2}{\rho_2-\rho_1}$.

By using the same methods for (3.45), (3.45) can be written as

$$t(u_1 - u_2)(E_2 - E_1) = \sigma_2 u_2 - \sigma_1 u_1. \tag{3.49}$$

Because of $E = e + \frac{1}{2}u^2$, we can get

$$e_2 - e_1 = -\frac{\sigma_1 + \sigma_2}{2t}. \tag{3.50}$$

Using the EOS of Mie-Grüneisen (2.4), can get

$$e = c_0 p - c_1 f(\rho/\rho_0), \tag{3.51}$$

where $c_0 = \frac{1}{\rho_0\Gamma_0}$ and $c_1 = \frac{a_0^2}{\Gamma_0}$. Put the above equation into (3.50), we can solve the pressure p_2 out as a function of ρ_2.

$$p_2 = \frac{2t(c_1 f(\rho_2/\rho_0) + e_1) - (\sigma_1 + s_{xx2})}{2tc_0 - 1}. \tag{3.52}$$

Thanks to (3.13), s_{xx2} can be written as

$$s_{xx2} = s_{xx1} - \frac{4}{3}\mu \ln(\frac{\rho_2}{\rho_1}). \tag{3.53}$$

Then, the Cauchy stress can be written as

$$\sigma_2 = -p_2 + s_{xx2}. \tag{3.54}$$

Then we can use (3.48) to solve the velocity after the shock

$$u_2 = \begin{cases} u_1 - \sqrt{\dfrac{\sigma_1 - \sigma_2}{t}} & \text{Left-going,} \\ u_1 + \sqrt{\dfrac{\sigma_1 - \sigma_2}{t}} & \text{Right-going.} \end{cases} \tag{3.55}$$

And the shock speed is given as

$$s = \frac{\rho_2 u_2 - \rho_1 u_1}{\rho_2 - \rho_1}. \tag{3.56}$$

By the above deductions for the moving shock wave, we can find that, if the density after the shock is known, all the data after the shock can be solved out.

3.2 Plastic state

When the material is yielding,

$$|s_{xx}| = \frac{2}{3}Y_0, \tag{3.57}$$

the equations of Riemann problem can be written as

$$\begin{cases} \partial_t \rho + \partial_x(\rho u) = 0, \\ \partial_t(\rho u) + \partial_x(\rho u^2 + p - s_{xx}) = 0, \\ \partial_t(\rho E) + \partial_x\left[(\rho E + p - s_{xx})u\right] = 0, \\ |s_{xx}| = \dfrac{2}{3}Y_0, \\ U(x, t=0) = \begin{cases} U_L, \text{ if } x < 0, \\ U_R, \text{ if } x \geq 0, \end{cases} \end{cases} \tag{3.58}$$

where $\mathbf{U} = (\rho, \rho u, \rho E)$.

3.2.1 Jacobian matrix in plastic regions

The motion equations of (3.58) can be written as

$$\partial_t \mathbf{U} + \mathbf{J}_p(\mathbf{U})\partial_x \mathbf{U} = 0, \tag{3.59}$$

where the Jacobian matrix is

$$\mathbf{J}_p(\mathbf{U}) = \begin{bmatrix} 0 & 1 & 0 \\ -u^2 + \frac{\partial p}{\partial \rho} + \Gamma(\frac{u^2}{2} - e) & u(2-\Gamma) & \Gamma \\ (\Gamma(\frac{u^2}{2} - e) - e - \frac{u^2}{2} + \frac{\sigma}{\rho} + \frac{\partial p}{\partial \rho})u + \frac{u^2}{2} & -\Gamma u^2 - \frac{\sigma}{\rho} + e & (1+\Gamma)u \end{bmatrix}. \tag{3.60}$$

The eigenvalues of $\mathbf{J}_p(\mathbf{Q})$ are given as

$$\lambda_1 = u, \quad \lambda_2 = u - c_p, \quad \lambda_3 = u + c_p,$$

where

$$c_p = \sqrt{a^2 - \frac{\rho_0}{\rho^2}\Gamma_0 s_{xx}}. \tag{3.61}$$

The corresponding right eigenvectors are

$$r_1 = \begin{bmatrix} -\frac{\Gamma}{b_1} \\ -\frac{\Gamma u}{b_1} \\ 1 \end{bmatrix}, \quad r_2 = \frac{1}{h - uc_p}\begin{bmatrix} 1 \\ u - c_p \\ h - uc_p \end{bmatrix}, \quad r_3 = \frac{1}{h + uc_p}\begin{bmatrix} 1 \\ u + c_p \\ h + uc_p \end{bmatrix}. \tag{3.62}$$

Comparing Eq.(3.6) with Eq.(3.61), we notice that the sonic speed is not continuous between the states of elastic and plastic. As the shear modulus μ is always positive, so the elastic wave runs always faster than the plastic wave.

3.2.2 Relations across the contact wave

According to the eigenvectors in Eq.(3.62), for the λ_1-wave ($\lambda_1 = u$), we have

$$\frac{d\rho}{\frac{-\Gamma}{b_1}} = \frac{d(\rho u)}{\frac{-u\Gamma}{b_1}} = \frac{d(\rho E)}{1}. \tag{3.63}$$

From the above equations, we can easily deduce that

$$du = 0, \quad dp = 0, \tag{3.64}$$

which means that

$$u_L^* = u_R^*, \quad p_L^* = p_R^*. \tag{3.65}$$

Because $s_{xxL}^* = s_{xxR}^*$, thanks to (2.3), one can get

$$\sigma_L^* = \sigma_R^*. \tag{3.66}$$

For convenience, we define

$$s^* = u_L^* = u_R^*. \tag{3.67}$$

3.2.3 Relations across rarefaction waves

Left-going rarefaction wave Across the left wave associated with λ_2-wave, ($\lambda_2 = u - c_p$), we have

$$\frac{d\rho}{1} = \frac{d(\rho u)}{u - c_p} = \frac{d(\rho E)}{h - uc_p}. \tag{3.68}$$

Samilar to section 3.1.4, we can get the relations

$$pe^{\frac{\lambda}{\rho}} - \int f_2(\rho)e^{\frac{\lambda}{\rho}} d\rho = \text{constant}. \tag{3.69}$$

and

$$u + \int \frac{c_p}{\rho} d\rho = \text{constant}. \tag{3.70}$$

Right-going rarefaction wave Across the right wave associated with λ_3-wave, ($\lambda_3 = u + c_e$), we have

$$\frac{d\rho}{1} = \frac{d(\rho u)}{u + c_p} = \frac{d(\rho E)}{h + uc_p}. \tag{3.71}$$

We can get similar relations as the left-going wave as

$$pe^{\frac{\lambda}{\rho}} - \int f_2(\rho)e^{\frac{\lambda}{\rho}} d\rho = \text{constant}. \tag{3.72}$$

$$u - \int \frac{c_p}{\rho} d\rho = \text{constant}. \tag{3.73}$$

3.2.4 Relations across a shock wave

By using the same deducing process as Section 3.1.5, we can get the states after the shock wave as

$$s_{xx2} = s_{xx1}, \tag{3.74}$$

$$p_2 = \frac{2t(c_1 f(\rho_2/\rho_0) + e_1) - (\sigma_1 + s_{xx2})}{2tc_0 - 1}, \tag{3.75}$$

where $c_0 = \frac{1}{\rho_0 \Gamma_0}$, $c_1 = \frac{a_0^2}{\Gamma_0}$, $\sigma_2 = -p_2 + s_{xx2}$,

$$u_2 = \begin{cases} u_1 - \sqrt{\dfrac{\sigma_1 - \sigma_2}{t}} & \text{Left-going,} \\ u_1 + \sqrt{\dfrac{\sigma_1 - \sigma_2}{t}} & \text{Right-going.} \end{cases} \tag{3.76}$$

And the shock speed is given as

$$s = \frac{\rho_2 u_2 - \rho_1 u_1}{\rho_2 - \rho_1}. \tag{3.77}$$

4 Exact Riemann solver

Now we consider the constructing details of the exact Riemann solver. For the Riemann problem in Section **??**, there are 6×6 possible cases in the Riemann solution with different wave structures. The left six cases are shown in Fig.1.

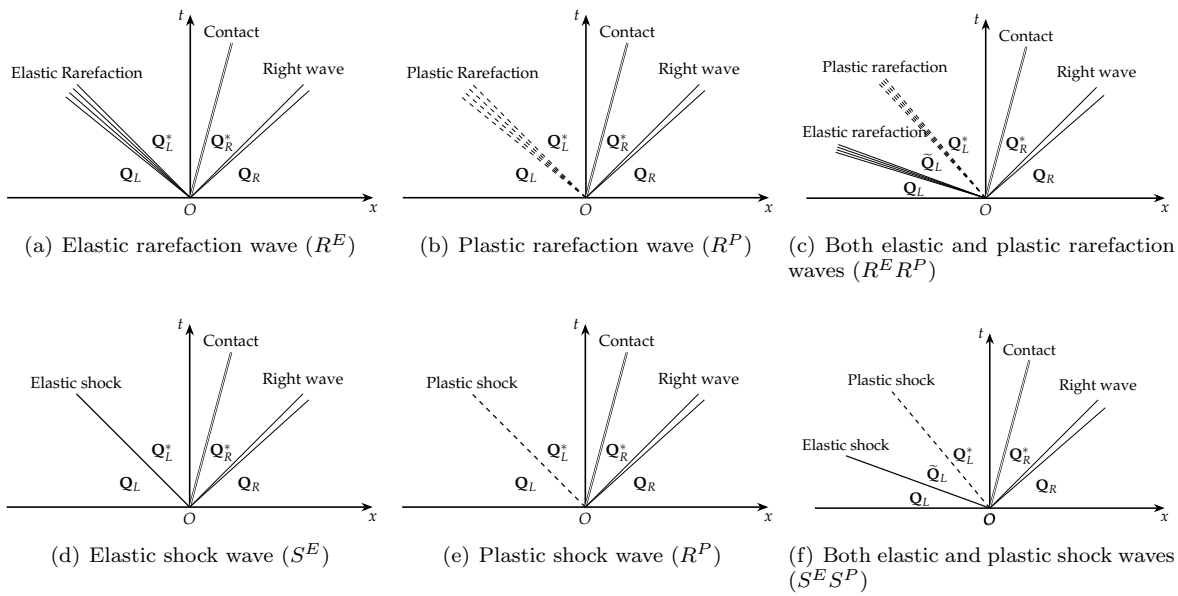

(a) Elastic rarefaction wave (R^E)

(b) Plastic rarefaction wave (R^P)

(c) Both elastic and plastic rarefaction waves ($R^E R^P$)

(d) Elastic shock wave (S^E)

(e) Plastic shock wave (R^P)

(f) Both elastic and plastic shock waves ($S^E S^P$)

Figure 1: The possible cases of Riemann solution structures in the left side.

4.1 The solving process

From Section 3, we can find that all variables can be formulated in terms of density. So we define equations

$$\begin{cases} f_u(\rho_L^*, \rho_R^*, \mathbf{Q}_L, \mathbf{Q}_R) = u_L^*(\rho_L^*, \mathbf{Q}_L) - u_R^*(\rho_R^*, \mathbf{Q}_R), \\ f_\sigma(\rho_L^*, \rho_R^*, \mathbf{Q}_L, \mathbf{Q}_R) = \sigma_L^*(\rho_L^*, \mathbf{Q}_L) - \sigma_R^*(\rho_R^*, \mathbf{Q}_R). \end{cases} \tag{4.1}$$

By using the relations across the contact wave in Section 3.1.3 and Section 3.2.2, we can get

$$\begin{cases} f_u(\rho_L^*, \rho_R^*, \mathbf{Q}_L, \mathbf{Q}_R) = u_L^*(\rho_L^*, \mathbf{Q}_L) - u_R^*(\rho_R^*, \mathbf{Q}_R) = 0, \\ f_\sigma(\rho_L^*, \rho_R^*, \mathbf{Q}_L, \mathbf{Q}_R) = \sigma_L^*(\rho_L^*, \mathbf{Q}_L) - \sigma_R^*(\rho_R^*, \mathbf{Q}_R) = 0. \end{cases} \tag{4.2}$$

Obviously, this system is uniquely solvable, but we can not get the analytical solution of (4.2). We have to use an iteration procedure to solve (4.2) and the solving process is shown in Fig.2. The details are introduced in the following.

Initial:

The initial densities are given as

$$\rho_{L(1)}^* = \frac{\rho_L + \rho_R}{2} \quad \rho_{R(1)}^* = \frac{\rho_L + \rho_R}{2}. \tag{4.3}$$

Iteration begin:

Step 1 Determining the case of the wave structure:

Given $\rho_{L(k)}^*$ and a $\rho_{R(k)}^*$ in the k-th iteration step, we can use the methods introduced in Section 4.2 to determine the case of wave structure of this Riemann problem. In this procedure for solving this Riemann problem, the subscript (k) means the variable in the k-th iteration step.

Step 2 Evaluating $f_{u(k)}$ and $f_{\sigma(k)}$:

After determining the structure case, we need to solve the Cauchy stresses and the velocities in regions $\mathbf{Q}_L^*$ and $\mathbf{Q}_R^*$, those are given in Section 4.4.

Step 3 Evaluating the derivatives of $f_{u(k)}$ and $f_{\sigma(k)}$.

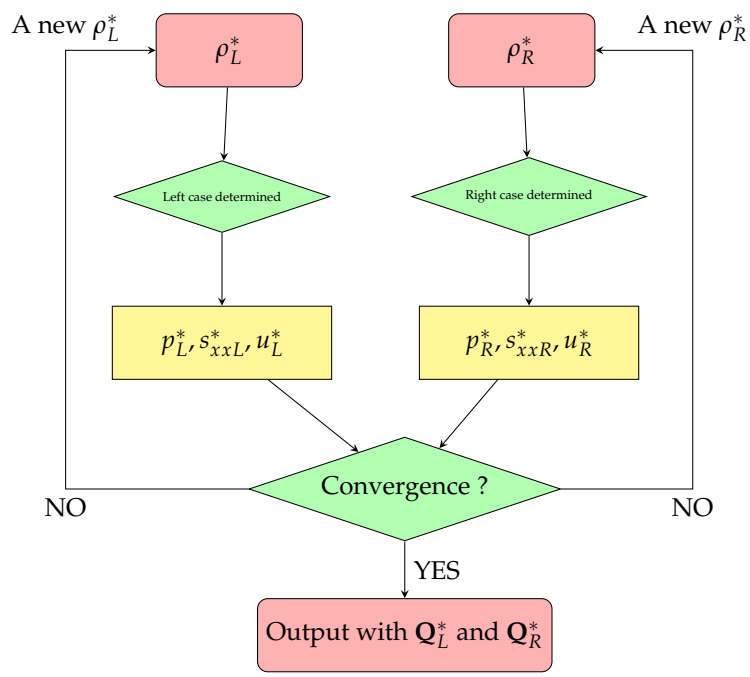

Figure 2: A flow chat of the Newton iteration process.

The derivatives of $f_{u(k)}$ and $f_{\sigma(k)}$ are given as

$$\frac{\partial f_{u(k)}}{\partial \rho_{L(R)}^*} = \frac{f_{u(k)} - f_{u(k-1)}}{\rho_{L(R)(k)}^* - \rho_{L(R)(k-1)}}, \quad \frac{\partial f_{\sigma(k)}}{\partial \rho_{L(R)}^*} = \frac{f_{\sigma(k)} - f_{\sigma(k-1)}}{\rho_{L(R)(k)}^* - \rho_{L(R)(k-1)}}. \tag{4.4}$$

At the first step, we use a simple numerical difference method

$$\frac{\partial f_{u(1)}}{\partial \rho_{L(R)}^*} = \frac{f_u(\rho_{L(R)}^* + \Delta\rho) - f_u(\rho_{L(R)}^*)}{\Delta\rho_{L(R)}}, \quad \frac{\partial f_{u(1)}}{\partial \rho_{L(R)}^*} = \frac{f_u(\rho_{L(R)}^* + \Delta\rho) - f_u(\rho_{L(R)}^*)}{\Delta\rho_{L(R)}}, \tag{4.5}$$

where $\Delta\rho$ is a little quantity, we define

$$\Delta\rho = \frac{\rho_{L(R)(1)}^*}{100}. \tag{4.6}$$

Step 4 Evaluating $\rho_{L(k+1)}^*$ and $\rho_{R(k+1)}^*$:

$$\begin{bmatrix} \rho_{L(k+1)}^* \\ \rho_{R(k+1)}^* \end{bmatrix} = \begin{bmatrix} \rho_{L(k)}^* \\ \rho_{R(k)}^* \end{bmatrix} - \begin{bmatrix} \frac{\partial f_{u(k)}}{\partial \rho_L^*} & \frac{\partial f_{u(k)}}{\partial \rho_R^*} \\ \frac{\partial f_{\sigma(k)}}{\partial \rho_L^*} & \frac{\partial f_{\sigma(k)}}{\partial \rho_R^*} \end{bmatrix}^{-1} \begin{bmatrix} f_{u(k)} \\ f_{\sigma(k)} \end{bmatrix} \tag{4.7}$$

Step 5 Convergence test:

The iteration is convergent if

$$\mathrm{CHA} \leq \mathrm{TOL}, \tag{4.8}$$

where

$$\mathrm{CHA} = \max\left[\frac{|\rho_{L(k+1)}^* - \rho_{L,(k)}^*|}{\frac{1}{2}|\rho_{L(k+1)}^* + \rho_{L(k)}^*|}, \frac{|\rho_{R(k+1)}^* - \rho_{R,(k)}^*|}{\frac{1}{2}|\rho_{R(k+1)}^* + \rho_{R(k)}^*|}, |f_u|, |f_\sigma|\right], \tag{4.9}$$

$$\mathrm{TOL} = 10^{-4}.$$

If not, go to Step 1 and continue the iteration procedure until convergent. Numerical examples show, after 2-4 iterations, the condition (4.8) is satisfied.

Iteration end

Table 4.1: The condition of cases classification.

$\hat{\rho^*} < \rho$	$\hat{s}_{xx} < \frac{2}{3}Y_0$ case a: R^E	$s_{xx} = \frac{2}{3}Y_0$ and $\hat{s}_{xx} \geq \frac{2}{3}Y_0$ case b: R^P	other case c: $R^E R^P$
$\hat{\rho^*} > \rho$	$\hat{s}_{xx} > -\frac{2}{3}Y_0$ case d: S^E	$s_{xx} = -\frac{2}{3}Y_0$ and $\hat{s}_{xx} \leq -\frac{2}{3}Y_0$ case e: S^P	other case f: $S^E S^P$

4.2 Determining the case of structures

Given the value of density $\rho^*_{L(R)}$, we can distinguish the non-linear wave is a shock or rarefaction wave. This is done easily by comparing $\rho^*_{L(R)}$ with $\rho_{L(R)}$, the subscript $_{L(R)}$ means in the left(right) side of the contact wave.

$$\begin{cases} \text{a rarefaction wave:} & \text{if } \rho_{L(R)} > \rho^*_{L(R)}, \\ \text{a shock wave:} & \text{if } \rho_{L(R)} < \rho^*_{L(R)}. \end{cases} \tag{4.10}$$

Thanks to (3.13), the deviatoric stress can be evaluated as

$$\hat{s}_{xxL(R)} = -\frac{4}{3}\mu \ln\left(\frac{\rho^*_{L(R)}}{\rho_{L(R)}}\right) + s_{xxL(R)}. \tag{4.11}$$

According to the values of initial and evaluated deviatoric stresses in (4.11) in one side of the contact wave, the non-linear wave in this side may be:

$$\begin{cases} \text{an elastic rarefaction} & \text{if } \hat{s}_{xxL(R)} < \frac{2}{3}Y^0, \\ \text{a plastic rarefaction} & \text{if } s_{xxL(R)} = \frac{2}{3}Y^0 \text{ and } \hat{s}_{xxL(R)} \geq \frac{2}{3}Y_0, \\ \text{an elastic rarefaction and a following plastic rarefaction} & \text{if } s_{xxL(R)} < \frac{2}{3}Y^0 \text{ and } \hat{s}_{xxL(R)} \geq \frac{2}{3}Y_0, \\ \text{an elastic shock} & \text{if } \hat{s}_{xxL(R)} > -\frac{2}{3}Y_0, \\ \text{a plastic shock} & \text{if } s_{xxL(R)} = -\frac{2}{3}Y^0 \text{ and } \hat{s}_{xxL(R)} \leq -\frac{2}{3}Y_0, \\ \text{an elastic shock and a following plastic shock} & \text{if } s_{xxL(R)} > -\frac{2}{3}Y^0 \text{ and } \hat{s}_{xxL(R)} \leq -\frac{2}{3}Y_0. \end{cases} \tag{4.12}$$

Combining (4.10) and (4.12), we can find, in any side of the wave structure of this Riemann problem, there are six cases showed in Table 4.1, where capital letters "S" and "R" mean the shock and rarefaction wave, respectively; superscript letters "E" and "P" indicate the elastic or plastic state of a wave, respectively. Otherwise, the subscript L or R are omitted for simplification.

4.3 States in middle regions ($\tilde{\mathbf{Q}}_L$ and $\tilde{\mathbf{Q}}_R$)

Cases (R^E, R^P, S^E and S^P)

For cases (R^E, R^P, S^E and S^P) in Fig.1, the material is totally yielding or totally not yielding, there is no midlle state $\tilde{\mathbf{Q}}_{L(R)}$. For expression convenience, we let

$$(\tilde{\rho}_{L(R)}, \tilde{u}_{L(R)}, \tilde{p}_{L(R)}, \tilde{s}_{xx}) = (\rho_{L(R)}, u_{L(R)}, p_{L(R)}, s_{xxL(R)}), \tag{4.13}$$

Case ($R^E R^P$)

Using the methods introduced in the Section (3.1.4), we can easily deduce the formulation of all unknown variables after the rarefaction wave. Here we do not show the details of deduction.

For the case ($R^E R^P$), after the elastic rarefaction wave, the deviatoric stress achieves the elastic limit. Thanks to (4.10) and (4.12), one can easily deduce that

$$\tilde{s}_{xxL(R)} = \frac{2}{3}Y_0.$$

By using (3.13), the density in $\tilde{\mathbf{Q}}_{L(R)}$ is given as

$$\tilde{\rho}_{L(R)} = \rho_{L(R)}\exp\left(-\frac{Y_0}{2\mu} + \frac{3s_{xxL(R)}}{4\mu}\right).$$

From (3.35) and (3.41), for the case $(R^E R^P)$, the pressure is rearranged as

$$p(\rho) = p_{L(R)}e^{\frac{\lambda}{\rho_{L(R)}} - \frac{\lambda}{\rho}} + e^{-\frac{\lambda}{\rho}}\int_{\rho_{L(R)}}^{\rho} f_2(x)e^{\frac{\lambda}{x}}dx, \tag{4.14}$$

where

$$\lambda = \rho_0\Gamma_0 \quad f_2(\rho) = a_0^2\frac{\partial f}{\partial \eta} - \lambda\frac{s_{xx}(\rho)}{\rho^2},\ s_{xx}(\rho) = -\frac{4}{3}\mu\ln\left(\frac{\rho}{\rho_{L(R)}}\right) + s_{xxL(R)}. \tag{4.15}$$

Thanks to (3.36) and (3.42), for the rarefaction wave case $(R^E R^P)$, the velocity is given as

$$u(\rho) = \begin{cases} u_L - \displaystyle\int_{\rho_L}^{\rho}\frac{c_e(x)}{x}dx & \text{for the left-going rarefaction wave,} \\ u_R + \displaystyle\int_{\rho_R}^{\rho}\frac{c_e(x)}{x}dx & \text{for the right-going rarefaction wave,} \end{cases} \tag{4.16}$$

where the sonic speed

$$c_e(\rho) = \sqrt{a_0^2\frac{\partial f}{\partial \eta} + \frac{p(\rho)}{\rho^2}\rho_0\Gamma_0 - \frac{\rho_0}{\rho^2}\Gamma_0 s_{xx}(\rho) + \frac{4}{3}\frac{\mu}{\rho}}. \tag{4.17}$$

States in region $\tilde{\mathbf{Q}}_{L(R)}$ can be solved as

$$\tilde{p}_{L(R)} = p(\rho_{L(R)}), \quad \tilde{u}_{L(R)} = u(\rho_{L(R)}). \tag{4.18}$$

Remark: In (4.14) and (4.16), there are two integral terms. Obviously, because of the complexity of the EOS, we can not get the exact integral values. We have to use the numerical methods to approximate the two integral terms with high order of accuracy. The approximation methods are introduced in the Appendix 1.

Case $(S^E S^P)$

Using the methods introduced in the Section (3.1.5), we can easily deduce the formulation of all unknown variables in $\tilde{\mathbf{Q}}_{L(R)}$. In order to shorten the length of our paper, we do not show the details of the deduction.

For the case $(S^E S^P)$, after the elastic shock wave, the deviatoric stress achieves the elastic limit. So, by using (4.10) and (4.12), one can easily deduce that

$$\tilde{s}_{xxL(R)} = -\frac{2}{3}Y_0.$$

From (3.13), after the elastic shock wave, the density in $\tilde{\mathbf{Q}}_{L(R)}$ is given as

$$\tilde{\rho}_{L(R)} = \rho_{L(R)}\exp\left(\frac{Y_0}{2\mu} + \frac{3s_{xxL(R)}}{4\mu}\right).$$

By using (3.52), the pressure can be solved as

$$\tilde{p}_{L(R)} = \frac{2t(c_1 f(\tilde{\rho}_{L(R)}/\rho_0) + e_{L(R)}) - (\sigma_{L(R)} + \tilde{s}_{xxL(R)})}{2tc_0 - 1}, \tag{4.19}$$

where $c_0 = \frac{1}{\rho_0\Gamma_0}$, $c_1 = \frac{a_0^2}{\Gamma_0}$ and $t = \frac{\rho_{L(R)}\tilde{\rho}_{L(R)}}{\tilde{\rho}_{L(R)} - \rho_{L(R)}}$.

Thanks to (3.55), the velocity can be written as

$$\begin{cases} \tilde{u}_L = u_L - \sqrt{\frac{\sigma_L - \tilde{\sigma}_L}{t}}, \\ \tilde{u}_R = u_R + \sqrt{\frac{\sigma_R - \tilde{\sigma}_R}{t}}, \end{cases} \tag{4.20}$$

where

$$\tilde{\sigma}_{L(R)} = -\tilde{p}_{L(R)} + \tilde{s}_{xxL(R)}. \tag{4.21}$$

4.4 States in regions $\mathbf{Q}_L^*$ and $\mathbf{Q}_R^*$

Rarefaction wave For rarefaction wave, we not only need to solve the state after the wave in region $\mathbf{Q}_{L(R)}^*$, but also need to know states inside the expansion region.

First we give the function of s_{xx},

$$s_{xx}(\rho) = \begin{cases} -\frac{4}{3}\mu \ln\left(\frac{\rho}{\tilde{\rho}_{L(R)}}\right) + s_{xxL(R)}, & \tilde{\rho}_{L(R)} \geq \rho \geq \rho_{L(R)}^*, \quad \text{case (a)}, \\ \frac{2}{3}Y_0, & \tilde{\rho}_{L(R)} \geq \rho \geq \rho_{L(R)}^*, \quad \text{case (b,c)}. \end{cases} \tag{4.22}$$

Then we give the pressure,

$$p(\rho) = \tilde{p}_{L(R)} e^{\frac{\lambda}{\rho_{L(R)}} - \frac{\lambda}{\rho}} + e^{-\frac{\lambda}{\rho}} \int_{\tilde{\rho}_{L(R)}}^{\rho} f_2(x) e^{\frac{\lambda}{x}} dx, \quad \tilde{\rho}_{L(R)} \geq \rho \geq \rho_{L(R)}^* \tag{4.23}$$

where

$$\lambda = \rho_0 \Gamma_0 \quad f_2(\rho) = a_0^2 \frac{\partial f}{\partial \eta} - \lambda \frac{s_{xx}(\rho)}{\rho^2}. \tag{4.24}$$

And sonic speed,

$$c(\rho) = \begin{cases} \sqrt{a_0^2 \frac{\partial f}{\partial \eta} + \frac{p(\rho)}{\rho^2}\rho_0\Gamma_0 - \frac{\rho_0}{\rho^2}\Gamma_0 s_{xx}(\rho) + \frac{4}{3}\frac{\mu}{\rho}} & \text{case (a)}, \\ \sqrt{a_0^2 \frac{\partial f}{\partial \eta} + \frac{p(\rho)}{\rho^2}\rho_0\Gamma_0 - \frac{\rho_0}{\rho^2}\Gamma_0 s_{xx}(\rho)} & \text{case (b,c)}. \end{cases} \tag{4.25}$$

Then we can get the function of velocity

$$u(\rho) = \begin{cases} \tilde{u}_L - \int_{\rho_L}^{\rho} \frac{c(x)}{x} dx, & \tilde{\rho}_L \geq \rho \geq \rho_L^*, \\ \tilde{u}_R + \int_{\rho_R}^{\rho} \frac{c(x)}{x} dx, & \tilde{\rho}_R \geq \rho \geq \rho_R^*, \end{cases} \tag{4.26}$$

By now, we can get the state in star regions as

$$p_{L(R)}^* = p(\rho_{L(R)}^*), \quad s_{xxL(R)}^* = s_{xx}(\rho_{L(R)}^*), \quad u_{L(R)}^* = u(\rho_{L(R)}^*). \tag{4.27}$$

Shock wave For shock waves, the deviatoric stress is given as

$$s_{xx}(\rho) = \begin{cases} -\frac{4}{3}\mu \ln\left(\frac{\rho}{\tilde{\rho}_{L(R)}}\right) + \tilde{s}_{xxL(R)}, & \text{case (d)}, \\ -\frac{2}{3}Y_0, & \text{cases (e, f)}. \end{cases} \tag{4.28}$$

And the pressure is given as

$$p(\rho) = \frac{2t(c_1 f(\rho/\rho_0) + \tilde{e}_{L(R)}) - (\tilde{\sigma}_{L(R)} + s_{xx}(\rho))}{2tc_0 - 1}, \tag{4.29}$$

where $c_0 = \frac{1}{\rho_0\Gamma_0}$ and $c_1 = \frac{a_0^2}{\Gamma_0}$ and $t = \frac{\tilde{\rho}_{L(R)}\rho}{\rho - \tilde{\rho}_{L(R)}}$. And the velocity is given as

$$u(\rho) = \begin{cases} \tilde{u}_L - \sqrt{\frac{\tilde{\sigma}_L - \sigma(\rho)}{t}}, \\ \tilde{u}_R + \sqrt{\frac{\tilde{\sigma}_R - \sigma(\rho)}{t}}, \end{cases} \tag{4.30}$$

where $\sigma(\rho) = -p(\rho) + s_{xx}(\rho)$. And the state in the star region is given as

$$p_{L(R)}^* = p(\rho_{L(R)}^*), \quad s_{xxL(R)}^* = s_{xx}(\rho_{L(R)}^*), \quad u_{L(R)}^* = u(\rho_{L(R)}^*). \tag{4.31}$$

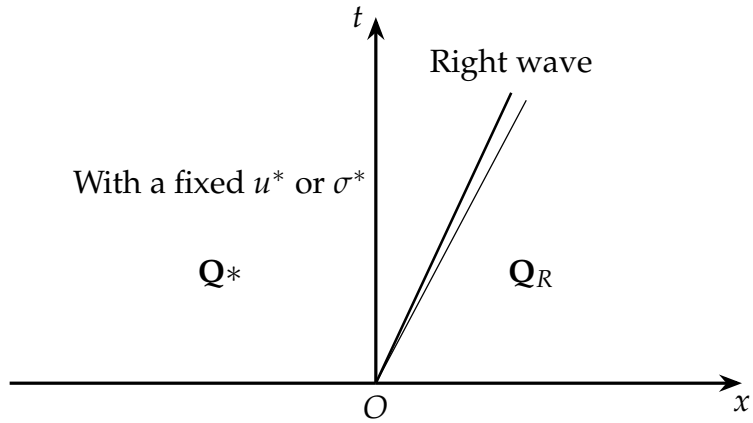

Figure 3: Half Riemann problem with a given left velocity or Cauchy stress..

5 Half Riemann problem and its solver

Some time we need to analyse a half Riemann problem with a given velocity or Cauchy stress. Shown in Fig.3 , in these cases, we only need to solve states in one side. There are six possible cases just like them in Section **??**.

As we know the velocity u^* or the Cauchy stress σ^*, there is only one function need to be solved as

$$f(\rho^*) = u(\rho^*) - u^* = 0, \tag{5.1}$$

or

$$f(\rho^*) = \sigma(\rho^*) - \sigma^* = 0. \tag{5.2}$$

The solving process is list in the following.

Initial:

The initial density is given as

$$\rho^*_{(0)} = \rho_R. \tag{5.3}$$

Iteration begin:

Step 1 Case select: By a given $\rho^*_{(k)}$ in k iteration step, we need to determine the case of the wave structures in the left side. The determining process is also done in Section 4.2.

Step 2 Solving f: After determining the structure case, we need to solve the velocity (or the Cauchy stress) in the region $\mathbf{Q}^*$, this is given in Section 4.4.

Step 3 Updating ρ^*: By the Newton iteration equation, a new density can be updated as

$$\rho^*_{(k+1)} = \rho^*_{(k)} - f/\frac{\partial f_{(k)}}{\partial \rho}, \tag{5.4}$$

The derivatives of f is given by

$$\frac{\partial f_{(k+1)}}{\partial \rho^*} = \frac{f_{(k+1)} - f_{(k)}}{\rho^*_{(k+1)} - \rho^*_{(k)}}, \tag{5.5}$$

At the first step, we use a simple numerical difference method

$$\frac{\partial f_{(1)}}{\partial \rho^*} = \frac{f(\rho^* + \Delta\rho) - f(\rho^*)}{\Delta\rho}, \tag{5.6}$$

where $\Delta\rho$ is a little quatity, we can choose it as

$$\Delta\rho = \frac{\rho^*_{(0)}}{100}. \tag{5.7}$$

Figure 4: Comparison resutls for Test 1 with the structrures of $S^P|S^P$.

Figure 5: Comparison resutls for Test 1 with the structrures of $S^E S^P|S^P S^E$.

Step 4 Convergence test: The convergence is meassured by

$$\mathrm{CHA} = \max\left[\frac{|\rho^*_{(k+1)} - \rho^*_{(k)}|}{\frac{1}{2}|\rho^*_{(k+1)} + \rho^*_{(k)}|}, |f|\right]. \tag{5.8}$$

and the tolerance is taken as $\mathrm{TOL} = 10^{-4}$.

If $\mathrm{CHA} \leq \mathrm{TOL}$, the iteration ends. It usually takes 2-4 step to get a convergence result.

Iteration end.

6 Numerical tests

In this section, by choosing suitable initial conditions, we will solve the Riemann problem with several different structure cases in the solution. For simple expression, in figures, we use same representations as those in [**?**]. "|" means the contact wave, and capital letters "S" and "R" means the shock and rarefaction wave. Superscript letters "E" and "P" indicate the elastic or plastic state of a wave. Numerical results by the method in [**?**] is used to verified the correctness of the exact solution. In the following tests, the materials are taken as aluminium and copper. The parameters for the EOS and constitutive model for aluminum and copper are $(\rho_0, a_0, \Gamma_0, s, \mu)_{\mathrm{Al}} = (8930\mathrm{kg/m^3}, 3940\mathrm{m/s}, 2, 1.49, 2.76, 2.76\times10^{10}\mathrm{Pa})$ and $(\rho_0, a_0, \Gamma_0, s, \mu)_{\mathrm{copper}} = (2785\mathrm{kg/m^3}, 5328\mathrm{m/s}, 2, 1.338, 4.5\times10^{10}\mathrm{Pa})$, respectively. The computational domain is set to be $[0, 1m]$ with 800 cell points and the intial interface is located at $0.5m$, the terminal time is $t = 5\times10^{-5}s$.

6.1 Test 1

In this case, the material is yielding at both sides, so the solution structure has three wave with two plastic waves and one contact. The initial condition is

$$\begin{cases} \text{L: Al}, \quad \rho = 2785\mathrm{kg/m^3}, \quad u = 20\mathrm{m/s}, \quad p = 1.0\mathrm{Pa}, \quad s_{xx} = -2.0\times10^8\mathrm{Pa}, \\ \text{R: Al}, \quad \rho = 2785\mathrm{kg/m^3}, \quad u = 0\mathrm{m/s}, \quad p = 1.0\mathrm{Pa}, \quad s_{xx} = -2.0\times10^8\mathrm{Pa}, \end{cases} \tag{6.1}$$

It can be seen that the exact solution matches the numerical results very well in Fig.4.

6.2 Test 2

Next, we consider a case with yielding process at both sides, so the result has five waves. The initial condition is

$$\begin{cases} \text{L: Al}, \quad \rho = 2785\mathrm{kg/m^3}, \quad u = 800\mathrm{m/s}, \quad p = 1.0\mathrm{Pa}, \quad s_{xx} = 0.0\mathrm{Pa}, \\ \text{R: Al}, \quad \rho = 2785\mathrm{kg/m^3}, \quad u = 0\mathrm{m/s}, \quad p = 1.0\mathrm{Pa}, \quad s_{xx} = 0.0\mathrm{Pa}, \end{cases} \tag{6.2}$$

Shown in Fig.5, the exact solution matches the numerical results well generally, besides the under-cooling effect performed in the numerical results, but it is not considered in the designing of the exact Riemann solver.

6.3 Test 3

In this example, we test the elastic rarefaction waves case. In the structrues there is one elastic rarefaction wave on each side of the contace wave. The initial condition is given as

$$\begin{cases} \text{L: Al}, \quad \rho = 2785\mathrm{kg/m^3}, \quad u = -2.0\mathrm{m/s}, \quad p = 1.0^7\mathrm{Pa}, \quad s_{xx} = 0.0\mathrm{Pa}, \\ \text{R: Al}, \quad \rho = 2785\mathrm{kg/m^3}, \quad u = 2.0\mathrm{m/s}, \quad p = 1.0\times10^7\mathrm{Pa}, \quad s_{xx} = 0.0\mathrm{Pa}, \end{cases} \tag{6.3}$$

Figure 6: Comparison resutls for Test 3 with the structrures of $R^E|R^E$.

Figure 7: Comparison resutls for Test 4 with the structrures of $R^E R^P|R^P R^E$.

We can see that the results of the exact solution match the numerical results very well.

6.4 Test 4

Then we test another example with both elastic and plastic rarefaction waves on both sides. The initial condition is

$$\begin{cases} \text{L: Al}, \quad \rho = 2785\text{kg/m}^3, \quad u = -40\text{m/s}, \quad p = 1.0 \times 10^7\text{Pa}, \quad s_{xx} = 0.0\text{Pa}, \\ \text{R: Al}, \quad \rho = 2785\text{kg/m}^3, \quad u = 40\text{m/s}, \quad p = 1.0 \times 10^7\text{Pa}, \quad s_{xx} = 0.0\text{Pa}. \end{cases} \tag{6.4}$$

Results are shown in Fig.7, the results of the exact solver matches the numerical results very well.

6.5 Test 5

All the above four tests have symmetrical wave structrues, next we will test an example with different structrues on different sides. The initial condition is given as

$$\begin{cases} \text{L: Al}, \quad \rho = 2785\text{kg/m}^3, \quad u = 40\text{m/s}, \quad p = 1.0 \times 10^8\text{Pa}, \quad s_{xx} = -2.0 \times 10^8\text{Pa}, \\ \text{R: Al}, \quad \rho = 2785\text{kg/m}^3, \quad u = -40\text{m/s}, \quad p = 1.0 \times 10^2\text{Pa}, \quad s_{xx} = 0.0\text{Pa}. \end{cases} \tag{6.5}$$

In the Fig.8 shown in both the numerical and exact solutions, there is one plastic shock on the left side and both the elastic and plastic shocks exist on the right.

6.6 Test 6

In this test, we consider an example with zero initial velocities on both sides, driving by the gradient of the pressure, there are rarefaction waves producted into the higher pressure side and shock waves generated into the lower pressure side. The initial condition is given as

$$\begin{cases} \text{L: Al}, \quad \rho = 2785\text{kg/m}^3, \quad u = 0.0\text{m/s}, \quad p = 1.0 \times 10^{10}\text{Pa}, \quad s_{xx} = 0.0\text{Pa}, \\ \text{R: Al}, \quad \rho = 2785\text{kg/m}^3, \quad u = 0.0\text{m/s}, \quad p = 1.0 \times 10^2\text{Pa}, \quad s_{xx} = 0.0\text{Pa}. \end{cases} \tag{6.6}$$

Shown in Fig.12, we can see there are two shocks in the right side and two rarefaction waves on the left side.

6.7 Test 7

Now we will consider two multi-material tests with different materials on different sides. In this test, on the left side, a lighter material of aluminum with a velocity impacts to a heavier material of copper. The initial condition is given as

$$\begin{cases} \text{L: Al}, \quad \rho = 2785\text{kg/m}^3, \quad u = 40\text{m/s}, \quad p = 0.1\text{Pa}, \quad s_{xx} = 0.0\text{Pa}, \\ \text{R: Copper}, \quad \rho = 8930\text{kg/m}^3, \quad u = 0.0\text{m/s}, \quad p = 0.1\text{Pa}, \quad s_{xx} = 0.0\text{Pa}. \end{cases} \tag{6.7}$$

Show in the Fig.10, there is a large jump of density at the material interface and both elastic shock and plastic shock exist in each side of the interface. The exact Riemann solver can solve the Riemann problem with multi-materials very well comparing to the MHLLCEP approximate solver.

Figure 8: Comparison resutls for Test 5 with the structrures of $R^P|R^P R^E$.

Figure 9: Comparison resutls for Test 6 with the structrures of $R^E R^P | S^P S^E$.

Figure 10: Comparison results for Test 7 with structrures of $R^E R^P | R^P R^E$.

6.8 Test 8

At last, we test another multi-materials case, in this test the initial condtion is given as

$$\begin{cases} \text{L: Copper}, \quad \rho = 8930\text{kg/m}^3, \quad u = 0.0\text{m/s}, \quad p = 1.0 \times 10^{10}\text{Pa}, \quad s_{xx} = 0.0\text{Pa}, \\ \text{R: Al}, \quad \rho = 2785\text{kg/m}^3, \quad u = 0\text{m/s}, \quad p = 10.0\text{Pa}, \quad s_{xx} = 0.0\text{Pa}. \end{cases} \tag{6.8}$$

Shown in Fig.11, there are two rarefaction waves on the left side and two shocks on the right side, there is a discontinuity of pressure on the interface, and the Cauchy stress is continuous, which meets with the theoretical analysis.

6.9 Test 9

Then we give two tests of half Riemann problem, the first is with a given left velocity $u^* = -20\text{m/s}$, and the right initial condition is

$$\text{Copper}, \quad \rho = 8930\text{kg/m}^3, \quad u = 0.0\text{m/s}, \quad p = 0.1\text{Pa}, \quad s_{xx} = 0.0\text{Pa}. \tag{6.9}$$

In Fig.12, comparason results are given by the exact half Riemann solver and the numerical method. We can see that the exact solver can resolve both the elastic and plastic shock waves well.

6.10 Test 10

The second half Riemann case is with a given left Cauchy stress $\sigma^* = 0\text{Pa}$, and the right initial condition is

$$\text{Copper}, \quad \rho = 8930\text{kg/m}^3, \quad u = 0.0\text{m/s}, \quad p = 1.0 \times 10^9\text{Pa}, \quad s_{xx} = 0.0\text{Pa}. \tag{6.10}$$

In Fig.13, we give the results computed by the exact Riemann solver and the numerical simulation, shown in it, the exact solver can resolve the elastic and plastic rarefaction waves well.

7 Results

In this paper, we give a detailed analysis of the Riemann problem for one-dimensional multi-material elastic-plastic flows with the Mie-Grüneisen EOS, hypo-elastic constitutive model and the von Mises' yielding condition. Some useful results are found through the analysing:

1. The sonic speed periods a significant jump when the material is yielding.
2. the plastic wave is always faster than the elastic wave for the reason of the sonic speed jump.
3. There are only thirty-six possible cases of the structrues in the Riemann problem.
4. All the variables after the wave can be written as functions of the density theoretically.

Then, based on the analysis, we have constructed exact Riemann solvers for both the Riemann problem and the half Riemann problem, separately. Tested by a large number of examples, the exact Riemann solver is reasonable and matching well with the numerical method for both single material problems and multi-material Riemann problems.

Figure 11: Comparison results for Test 8 with the structrures of $R^E R^P | S^E S^P$.

Figure 12: Comparison results for Test 9 with the structrures of $S^E S^P$.

Figure 13: Comparison results for Test 10 with the structrures of $R^E R^P$.

Acknowledgement

r This work was supported by NSFC(Grant No. 11672047) and Science Challenge Project (Grant No. TZ2016002).

A Gauss-Legendre quadrature

In this paper, we use Gauss-Legendre quadrature to take numerical integrations. For a function $f(x)$, the intergration from -1 to 1 is given as

$$\int_{-1}^{1} f(x)dx \approx \sum_{i=0}^{n} \omega_i f(p_i)$$

ω_i is the weight, and p_i is the integrating point. For different orders they are listed in Table A

Table A.1: Coefficiences for Guass-Legendere quadrature

Number of points, n	Order	Points, x_i	Weights, ω_i
1	1	0	2
2	3	$\pm\frac{1}{\sqrt{3}}$	1
3	3	0	$\frac{8}{9}$
		$\pm\sqrt{\frac{3}{5}}$	$\frac{5}{9}$
4	7	$\pm\sqrt{\frac{3}{7}-\frac{2}{7}\sqrt{\frac{6}{5}}}$	$\frac{18+\sqrt{30}}{36}$
		$\pm\sqrt{\frac{3}{7}+\frac{2}{7}\sqrt{\frac{6}{5}}}$	$\frac{18-\sqrt{30}}{36}$